Available online at www.sciencedirect.com
SCIENCE DIRECT®
Comput. Methods Appl. Mech. Engrg. 195 (2006) 1778–1792
Computer methods in applied mechanics and engineering
www.elsevier.com/locate/cma

A dynamic multiscale viscosity method for the spectral approximation of conservation laws

Assad A. Oberai *, John Wanderer

Department of Aerospace and Mechanical Engineering, Boston University, Boston, 110 Cummington Street, MA 02215, USA

Received 10 September 2004; received in revised form 15 February 2005; accepted 26 May 2005

Dedicated to Prof. Thomas J.R. Hughes on the occasion of his 60th birthday

Abstract

We consider the spectral approximation of a conservation law in the limit of small or vanishing viscosities. In this regime, the continuous solution of the problem is known to develop sharp spatial and temporal gradients referred to as shocks. Also, the standard Fourier–Galerkin solution is known to break down if the mesh parameter is larger than the shock width. In this paper we propose a new dynamic, multiscale viscosity method which enables the solution of such systems with relatively coarse discretizations. The key features of this method are: (1) separate viscosities are applied to the coarse and the fine scale equations; (2) these viscosities are determined as a part of the calculation (dynamically) from a consistency condition which must be satisfied if the resulting numerical solution is optimal in a user-defined sense. In this paper we develop these conditions, and demonstrate how they may be used to determine the numerical viscosities. We apply the proposed method to the one dimensional Burgers equation and note that it yields results that compare favorably with the vanishing spectral viscosity solution.

Keywords: Multiscale methods; Conservation laws; Spectral methods; Dynamic numerical methods; Numerical viscosity

1. Introduction

In this paper we develop a numerical method for the spectral approximation of non-linear conservation laws. These laws describe a broad range of physical phenomena which include the dynamics of gasses, the flow of traffic and the propagation of shallow water and non-linear acoustic waves. In all these systems we are interested in cases when the physical viscosity (or diffusivity) is small or zero. In the small viscosity case,

* Corresponding author. Tel.: +1 617 353 7381; fax: +1 617 353 5866.
E-mail address: oberai@bu.edu (A.A. Oberai).

0045-7825/$ - see front matter © 2005 Elsevier B.V. All rights reserved.
doi:10.1016/j.cma.2005.05.035

the solution to such systems develops local regions of large spatial and temporal gradients called shocks. The width of a shock reduces with reducing viscosity, and in the limit of zero viscosity the solution becomes discontinuous. In fact, in this limit in order to ensure unique solutions, the conservation law must be supplemented with an entropy production inequality and conditions that relate jumps in conserved quantities across the shock [1,2].

For small viscosities, the standard Fourier–Galerkin approximation to non-linear conservation laws becomes unstable if the shock width is smaller than the grid size. For a large class of problems the computational cost of employing a grid which is fine enough to resolve a shock is prohibitive and as a result this method finds limited application. Further, in the limit of zero viscosity, even with sufficient grid refinement, the Fourier–Galerkin solution does not converge to the unique "physical" solution which satisfies the entropy production inequality. To overcome these difficulties associated with the Fourier–Galerkin method, several methods have been proposed. A large proportion of these methods involve appending to the Fourier–Galerkin formulation a numerical viscosity term (see [3] for example). We choose to classify different numerical viscosity based methods on the basis of the equations in which the viscosity appears. To accomplish this, we introduce the concept of the *coarse* and the *fine scale equations* of a numerical approximation as follows.

In a Fourier–Galerkin method, the residual of the original partial differential equation is weighted by a Fourier mode, integrated over the domain, and the result is set to zero. This leads to a finite number of ordinary differential equations (ODEs), which may then be solved to determine the coefficients in the Fourier expansion of the numerical solution (see [4] for example). Note that in a Galerkin method the same set of modes is used for the weighting functions and the trial solution. Given a set of modes that comprises the weighting function space, we select a scalar $\tilde{k}$ and label modes with wave numbers k such that $|k| < \tilde{k}$ as the low wave number or the coarse scale modes, and the remaining modes as the high wave number or the fine scale modes. Then depending on whether an ODE in the numerical approximation is obtained from a coarse or a fine scale weighting function, we classify it as a coarse or a fine scale equation.

In several popular methods (such as the vanishing viscosity method [5]) that guarantee the convergence of the numerical solution to the unique entropy solution, the numerical viscosity is applied to both the coarse and the fine scale equations. On the other hand, in the vanishing spectral viscosity method proposed by Tadmor [6], the viscosity is applied only to the fine scale equations. As a result, this method retains the spectral accuracy of the coarse or the large scale modes while guaranteeing convergence to the entropy solution. It is interesting to note that in the context of the large eddy simulation (LES) of incompressible turbulent flows, the multiscale method of Hughes et al. [7,8], also involves applying a numerical viscosity only to the fine scale equations.

Motivated by the class of methods where the viscosity appears only in the fine scale equations, we propose a method where *different numerical viscosities appear in the large and the small scale equations*. In addition, in contrast to the methods described above, these viscosities are not determined a priori, instead they are calculated as part of the solution (dynamically). The equations that are used to determine the viscosities are derived from the condition that the resulting numerical method be optimal in a certain user-defined sense. We dub this method the dynamic multiscale viscosity method.

We remark that the equation used to dynamically determine the viscosities, is in effect the variational counterpart of the Germano identity. This identity has found widespread use in determining model parameters in the LES of turbulent flows [9]. Recently, we have demonstrated how it may be used as a tool for determining unknown parameters in a numerical method aimed at solving an abstract partial differential equation [10]. The work presented in this paper is an application of this methodology to the spectral approximation of non-linear conservation laws. In particular we use it to develop the dynamic multiscale method for a generic non-linear conservation law and then apply it to the model case of one-dimensional Burgers equation to study its properties. We find that the dynamic multiscale method outperforms the vanishing spectral viscosity method.

An outline of the remainder of this paper is as follows: In Section 2, we present the equations for a generic non-linear conservation law. In Section 3, we introduce its Fourier–Galerkin approximation. In Section 4, we introduce the multiscale viscosity method. In Section 5, we derive the necessary conditions that ensure the multiscale viscosity method is optimal in a user-defined sense. We employ these conditions in Section 6 to derive expressions for the multiscale viscosities. This completes the description of the dynamic multiscale method. In Section 7, we apply the proposed method to the one-dimensional Burgers equation, and compare the results with the Fourier–Galerkin and the spectral vanishing viscosity methods. We end with concluding remarks in Section 8.

2. Problem statement

We represent a generic non-linear conservation law with the following quasi-linear partial differential equation in the space-time domain $Q = \Omega \times]0, T[$, where $\Omega = [0, 2\pi]$ is the spatial domain, and $]0, T[$ denotes the time period of interest: Given $\boldsymbol{f}$, $\boldsymbol{G}$, $\boldsymbol{D}$ and $\boldsymbol{u}_0$, find $\boldsymbol{u} : Q \to \mathbb{R}^n$, such that

$$\boldsymbol{u}_{,t} + \boldsymbol{G}(\boldsymbol{u})_{,x} - \boldsymbol{D}\boldsymbol{u}_{,xx} + \boldsymbol{f} = \boldsymbol{0} \quad \text{in } Q, \tag{1}$$

$$\boldsymbol{u}(x, 0) = \boldsymbol{u}_0(x) \quad \text{in } \Omega. \tag{2}$$

In the equations above, $\boldsymbol{u}_{,t}$ is the time derivative of $\boldsymbol{u}$, $\boldsymbol{G} : \mathbb{R}^n \to \mathbb{R}^n$ is a non-linear vector function of $\boldsymbol{u}$, $\boldsymbol{D} : \mathbb{R}^n \to \mathbb{R}^n$ is an $n \times n$ positive semi-definite matrix of viscosities given by $\boldsymbol{D} = \operatorname{diag}\{v_1, \ldots, v_n\}$, and $\boldsymbol{u}_0$ is the initial condition. The form of Eqs. (1) and (2) is representative of a large class of physical phenomena that includes the dynamics of gasses, models of traffic flow, non-linear water waves, and processes described by Burgers equation.

We consider periodic boundary conditions for $\boldsymbol{u}$ expressed as

$$\boldsymbol{u}(2\pi, t) = \boldsymbol{u}(0, t), \quad t \in]0, T[. \tag{3}$$

For any $\boldsymbol{v} : Q \to \mathbb{R}^n$, we introduce a Fourier-series representation $\mathbb{P}^{(\alpha)}\boldsymbol{v}$, defined as

$$\mathbb{P}^{(\alpha)}\boldsymbol{v} = \sum_{0 \leqslant |k| \leqslant \alpha} \hat{\boldsymbol{v}}(k, t) \mathrm{e}^{\mathrm{i}kx}, \tag{4}$$

where k is the wave number, and $\hat{\boldsymbol{v}}$ are the Fourier coefficients given by

$$\hat{\boldsymbol{v}}(k, t) = \frac{1}{2\pi} \int_{\Omega} \boldsymbol{v}(x, t) \mathrm{e}^{-\mathrm{i}kx} \, \mathrm{d}x. \tag{5}$$

It is easily verified that the operator $\mathbb{P}^{(\alpha)}$ commutes with spatial and temporal differentiation and that

$$\mathbb{P}^{(\alpha)}\mathbb{P}^{(\beta)} = \mathbb{P}^{(\beta)}\mathbb{P}^{(\alpha)} = \mathbb{P}^{(\min(\alpha,\beta))}. \tag{6}$$

We will make use of this property in deriving the consistency conditions for the optimal numerical method in Section 5.

We are interested in spectral approximation of (1) and (2) for small viscosities ($|\boldsymbol{D}| \ll 1$) and in the limit of vanishing viscosities ($|\boldsymbol{D}| \to 0$). For small viscosities the solution to these equations is known to exhibit sharp variations in space and time called shocks. For $\boldsymbol{D} = \boldsymbol{0}$ the solution becomes discontinuous and multivalued. To ensure uniqueness, (1) and (2) must be supplemented with conditions that relate jumps in conserved quantities across a shock and an entropy production inequality. Another mechanism to arrive at the same physically relevant solution in this limit is to construct a solution with finite viscosity and then consider the limit $|\boldsymbol{D}| \to 0$.

3. Fourier–Galerkin approximation

The Fourier–Galerkin approximation of (1) and (2) is a function $\boldsymbol{u}^{(N)}$

$$\boldsymbol{u}^{(N)} = \sum_{0\leqslant|k|\leqslant N} \hat{\boldsymbol{u}}(k,t)\mathrm{e}^{\mathrm{i}kx} \tag{7}$$

such that

$$\mathbb{P}^{(N)}[\boldsymbol{u}^{(N)}_{,t} + \boldsymbol{G}(\boldsymbol{u}^N)_{,x} - \boldsymbol{D}\boldsymbol{u}^N_{,xx} + \boldsymbol{f}] = \boldsymbol{0} \quad \text{in } Q, \tag{8}$$

$$\mathbb{P}^{(N)}\boldsymbol{u}^{(N)}(x,0) = \mathbb{P}^{(N)}\boldsymbol{u}_0(x) \quad \text{in } \Omega. \tag{9}$$

Noting that $\mathbb{P}^{(N)}$ commutes with spatial and temporal differentiation, and that $\mathbb{P}^{(N)}\boldsymbol{u}^{(N)} = \boldsymbol{u}^{(N)}$, (8) and (9) may be simplified as

$$\boldsymbol{u}^{(N)}_{,t} + \left(\mathbb{P}^{(N)}[\boldsymbol{G}(\boldsymbol{u}^{(N)})]\right)_{,x} - \boldsymbol{D}\boldsymbol{u}^{(N)}_{,xx} + \mathbb{P}^{(N)}\boldsymbol{f} = \boldsymbol{0} \quad \text{in } Q, \tag{10}$$

$$\boldsymbol{u}^{(N)}(x,0) = \mathbb{P}^{(N)}\boldsymbol{u}_0(x) \quad \text{in } \Omega. \tag{11}$$

Using (7) in (10) and (11) and invoking the orthogonality of $\mathrm{e}^{\mathrm{i}kx}$ in Ω, we have

$$\hat{\boldsymbol{u}}^{(N)}_{,t} + \mathrm{i}k\hat{\boldsymbol{G}}(\boldsymbol{u}^{(N)}) + k^2\boldsymbol{D}\hat{\boldsymbol{u}}^{(N)} + \hat{\boldsymbol{f}} = \boldsymbol{0}, \quad 0 \leqslant |k| \leqslant N \text{ in }]0,T[, \tag{12}$$

$$\hat{\boldsymbol{u}}^{(N)}(k,0) = \hat{\boldsymbol{u}}_0(k), \quad 0 \leqslant |k| \leqslant N. \tag{13}$$

Note that in (12), for notational convenience, we have omitted the explicit dependence of the Fourier coefficients (the hat terms) on k and t.

Eqs. (10)–(13) are both expressions of the Fourier–Galerkin approximation to the original partial differential equation. We wish to solve these equations in the limit of small or vanishing viscosities when the mesh size denoted by π/N is much larger than the shock width. In this case, the Fourier–Galerkin is known to produce large spurious oscillations and become unstable. Further, in the limit $\boldsymbol{D} = \boldsymbol{0}$, even with mesh refinement, that is $N \to \infty$, the Fourier–Galerkin solution is known *not to* converge to "physical" entropy solution. In order to address these issues, in the following section we propose a multiscale method based on adding numerical viscosities to the Fourier–Galerkin approximation.

4. Multiscale viscosity method

We augment the Fourier–Galerkin method with *multiscale* viscosities. The choice of using two distinct viscosities, one for the coarse scale equations, and another for the fine scale equations is motivated by the earlier work of several researchers [6–8,11]. The resulting method is given by

$$\boldsymbol{u}^{(N)}_{,t} + \left(\mathbb{P}^{(N)}[\boldsymbol{G}(\boldsymbol{u}^{(N)})]\right)_{,x} - \left(\boldsymbol{D} + \frac{\bar{\boldsymbol{D}}}{N}\mathbb{P}^{(\alpha N)} + \frac{\acute{\boldsymbol{D}}}{N}(\mathbb{I} - \mathbb{P}^{(\alpha N)})\right)[\boldsymbol{u}^{(N)}_{,xx}] + \mathbb{P}^{(N)}\boldsymbol{f} = \boldsymbol{0} \quad \text{in } Q, \tag{14}$$

where $\alpha \in]0,1[$ is a real number, $\mathbb{I}$ is the identity operator, and $\bar{\boldsymbol{D}} = \mathrm{diag}\{\bar{\nu}_1, \ldots, \bar{\nu}_n\}$ and $\acute{\boldsymbol{D}} = \mathrm{diag}\{\acute{\nu}_1, \ldots, \acute{\nu}_n\}$ are matrices of numerical viscosities. The initial condition remains unaltered and is given by (11). Note that two distinct numerical viscosities, given by $\bar{\boldsymbol{D}}/N$ and $\acute{\boldsymbol{D}}/N$, appear in the equations for the coarse and fine scales, respectively. This is clearly seen once equations for the Fourier coefficients of $\boldsymbol{u}^{(N)}$ are evaluated. That is, using (7) in (14),

$$\hat{\boldsymbol{u}}_{N,t} + \mathrm{i}k\hat{\boldsymbol{G}}(\boldsymbol{u}^{(N)}) + k^2\left(\boldsymbol{D} + \frac{\bar{\boldsymbol{D}}}{N}\right)\hat{\boldsymbol{u}}^{(N)} + \hat{\boldsymbol{f}} = \boldsymbol{0}, \quad 0 \leqslant |k| \leqslant \alpha N \text{ in }]0, T[, \tag{15}$$

$$\hat{\boldsymbol{u}}_{N,t} + \mathrm{i}k\hat{\boldsymbol{G}}(\boldsymbol{u}^{(N)}) + k^2\left(\boldsymbol{D} + \frac{\acute{\boldsymbol{D}}}{N}\right)\hat{\boldsymbol{u}}^{(N)} + \hat{\boldsymbol{f}} = \boldsymbol{0}, \quad \alpha N < |k| \leqslant N \text{ in }]0, T[. \tag{16}$$

Since (15) is obtained from coarse scale weighting functions ($|k| \leqslant \alpha N$), and (16) is obtained from fine scale weighting functions we term these equations the *coarse and fine scale equations*, respectively. As is apparent from these equations, the numerical viscosity that appears in the coarse and fine scale equations is given by $\bar{\boldsymbol{D}}/N$ and $\acute{\boldsymbol{D}}/N$, respectively.

While the proposed method is motivated by earlier works (see [6–8,11]), there are two crucial differences:

1. In the aforementioned methods the viscosity is applied only to the fine scale equations. The viscosity in the coarse scale equations is zero. In our method different but non-zero viscosities are applied to both the coarse and the fine scale equations.
2. In the aforementioned methods the viscosity is determined a priori. In our method the viscosity is determined as a part of the calculation using an optimality argument. This development is described in the following section.

5. Consistency conditions

We now derive a set of consistency conditions that are utilized in the next section to compute an explicit expression for evaluating the numerical viscosities. These conditions are motivated by the Germano identity, which is commonly used to evaluate parameters in subgrid models for the large eddy simulation of turbulent flows [9].

The main idea which is expressed in Theorem 5.1 below, is the following. We assume that it is possible to choose the viscosities in (14) such that the resulting solution is optimal in the sense that its Fourier coefficients exactly match the corresponding coefficients of the continuous solution. Note that other, user-defined definitions of an optimal solution are also possible. In addition, we assume that the same viscosities also yield optimal results for a coarser discretization. That is the solution of (14) with N replaced by M everywhere, where $M < N$, is also optimal in the manner described above. These assumptions lead to a set of conditions that must be satisfied by the numerical viscosities in order to yield optimal results. A key feature of these conditions is that they do not involve the continuous solution $\boldsymbol{u}$, and are expressed entirely in terms of the numerical solution $\boldsymbol{u}^N$. Hence they may be utilized with relative ease to determine the numerical viscosities.

Theorem 5.1. *Let $\boldsymbol{u}^{(N)}$ and $\boldsymbol{u}^{(M)}$ be solutions of the multiscale viscosity method with modes up to N and M, respectively, with $M < N$. If*

$$\boldsymbol{u}^{(N)} = \mathbb{P}^{(N)}\boldsymbol{u}, \tag{17}$$

$$\boldsymbol{u}^{(M)} = \mathbb{P}^{(M)}\boldsymbol{u}, \tag{18}$$

where $\boldsymbol{u}$ is the solution of the continuous problem, then

$$\left(\bar{\boldsymbol{D}}\left(\frac{\mathbb{P}^{(\alpha M)}}{M} - \frac{\mathbb{P}^{(\alpha N)}}{N}\right) + \acute{\boldsymbol{D}}\left(\frac{\mathbb{I} - \mathbb{P}^{(\alpha M)}}{M} - \frac{\mathbb{I} - \mathbb{P}^{(\alpha N)}}{N}\right)\right)\left[\left(\mathbb{P}^{(M)}\boldsymbol{u}^{(N)}\right)_{,xx}\right]$$
$$= \left(\mathbb{P}^{(M)}\left[\boldsymbol{G}(\mathbb{P}^{(M)}\boldsymbol{u}^{(N)}) - \boldsymbol{G}(\boldsymbol{u}^{(N)})\right]\right)_{,x} \quad \text{in } Q. \tag{19}$$

Proof. $\boldsymbol{u}^{(M)}$ satisfies (14) with N replaced by M everywhere. Further, from (18)

$$\boldsymbol{u}^{(M)} = \mathbb{P}^{(M)}\boldsymbol{u} = \mathbb{P}^{(M)}\mathbb{P}^{(N)}\boldsymbol{u} \quad (\text{from (6), and since } M < N) = \mathbb{P}^{(M)}\boldsymbol{u}^{(N)} \quad (\text{from (17)}). \tag{20}$$

Using (20) in (14) written with N replaced by M, and rearranging terms so as to retain only the model term on the left-hand side, we arrive at

$$\begin{aligned}&\left(\frac{\bar{\boldsymbol{D}}}{M}\mathbb{P}^{(\alpha M)} + \frac{\acute{\boldsymbol{D}}}{M}(\mathbb{I} - \mathbb{P}^{(\alpha M)})\right)[(\mathbb{P}^{(M)}\boldsymbol{u}^{(N)})_{,xx}] \\ &\quad = \mathbb{P}^{(M)}\boldsymbol{u}^{(N)}_{,t} + \left(\mathbb{P}^{(M)}[\boldsymbol{G}(\mathbb{P}^{(M)}\boldsymbol{u}^{(N)})]\right)_{,x} - \boldsymbol{D}(\mathbb{P}^{(M)}\boldsymbol{u}^{(N)})_{,xx} + \mathbb{P}^{(M)}\boldsymbol{f} \quad \text{in } Q.\end{aligned} \tag{21}$$

By applying $\mathbb{P}^{(M)}$ to (14), assuming that $\mathbb{P}^{(M)}$ and spatial differentiation commute, using property (17), and rearranging terms so as to retain only the model term on the left-hand side, we conclude that

$$\begin{aligned}&\left(\frac{\bar{\boldsymbol{D}}}{N}\mathbb{P}^{(\alpha N)} + \frac{\acute{\boldsymbol{D}}}{N}(\mathbb{I} - \mathbb{P}^{(\alpha N)})\right)[(\mathbb{P}^{(M)}\boldsymbol{u}^{(N)})_{,xx}] \\ &\quad = \mathbb{P}^{(M)}\boldsymbol{u}^{(N)}_{,t} + \left(\mathbb{P}^{(M)}[\boldsymbol{G}(\boldsymbol{u}^{(N)})]\right)_{,x} - \boldsymbol{D}\mathbb{P}^{(M)}\boldsymbol{u}^{(N)}_{,xx} + \mathbb{P}^{(M)}\boldsymbol{f} \quad \text{in } Q.\end{aligned} \tag{22}$$

Subtracting (22) from (21) we have the desired result (viz. (19)). □

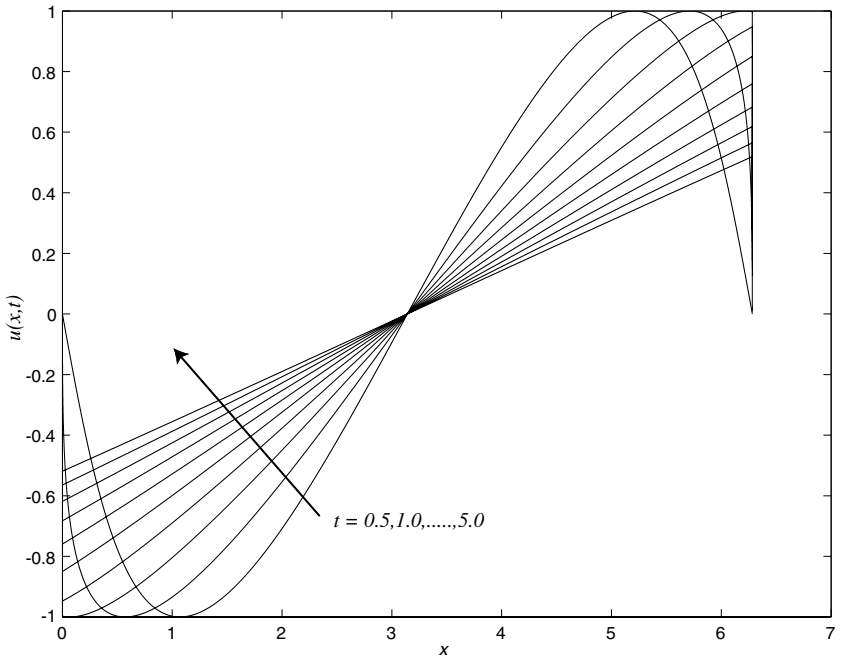

Fig. 1. Well resolved numerical solution (DNS) at $t = 0.5$, 1.0, 1.5, 2.0, 2.5, 3.0, 3.5, 4.0, 4.5 and 5.0 (arrow indicates increasing time).

Remark. The Fourier representation of (19) is given by

$$-k^2\left\{\begin{array}{ll}\left(\dfrac{\bar{\boldsymbol{D}}}{M}-\dfrac{\bar{\boldsymbol{D}}}{N}\right)(\hat{\boldsymbol{u}}^{(N)}), & 0\leqslant|k|\leqslant\alpha M\\ \left(\dfrac{\acute{\boldsymbol{D}}}{M}-\dfrac{\bar{\boldsymbol{D}}}{N}\right)(\hat{\boldsymbol{u}}^{(N)}), & \alpha M\leqslant|k|\leqslant\beta\\ \left(\dfrac{\acute{\boldsymbol{D}}}{M}-\dfrac{\acute{\boldsymbol{D}}}{N}\right)(\hat{\boldsymbol{u}}^{(N)}), & \beta\leqslant|k|\leqslant M\end{array}\right\}=\mathrm{i}k\Big(\hat{\boldsymbol{G}}(\mathbb{P}^{(M)}\boldsymbol{u}^{(N)})-\hat{\boldsymbol{G}}(\boldsymbol{u}^{(N)})\Big)\quad\text{in }]0,T[, \tag{23}$$

where

$$\beta=\min(\alpha N,M). \tag{24}$$

6. Evaluation of the viscosity parameters

Eq. (19) (or (23)) represents as many relations as there are modes for which $|k|\leqslant M$. We wish to evaluate only the $2n$ parameters that appear in $\bar{\boldsymbol{D}}$ and $\acute{\boldsymbol{D}}$ using these relations. One mechanism of reducing (19) to $2n$ equations is to equate the L_2 inner product of its residual with the linearly independent functions

$$\mathbb{P}^{(\alpha M)}u_j^{(N)},\quad j=1,\ldots,n \tag{25}$$

and

$$(\mathbb{I}-\mathbb{P}^{(\alpha M)})u_j^{(N)},\quad j=1,\ldots,n \tag{26}$$

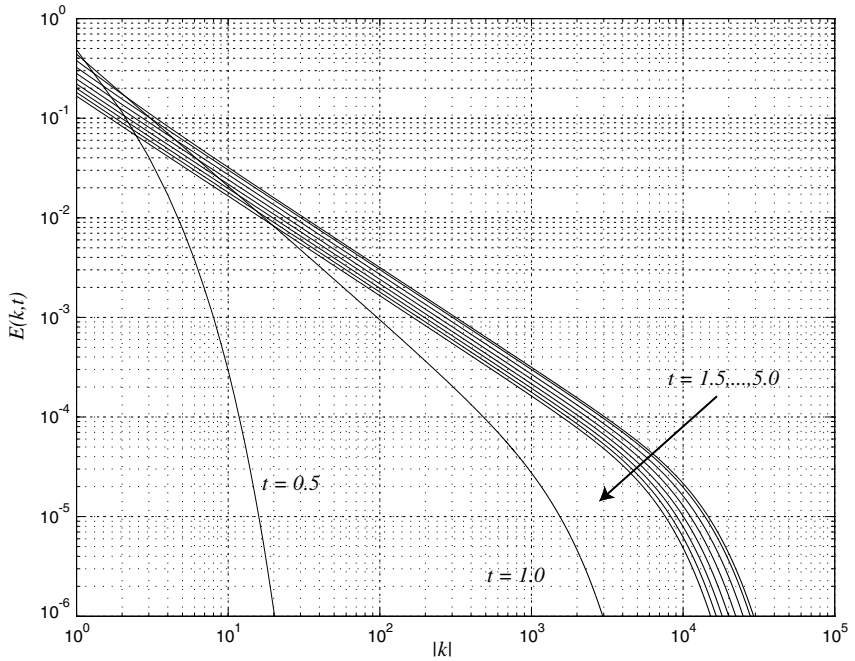

Fig. 2. $E(k)$ for the well resolved numerical solution (DNS) at $t=0.5$, 1.0, 1.5, 2.0, 2.5, 3.0, 3.5, 4.0, 4.5 and 5.0 (arrow indicates increasing time).

to zero. This procedure leads to $2n$ scalar equations that are most conveniently expressed in terms of the Fourier coefficients of $\boldsymbol{u}^{(N)}$. For $j = 1, \ldots, n$ they are given by

$$-\left(\frac{\bar{\nu}_j}{M} - \frac{\bar{\nu}_j}{N}\right) \sum_{0 \leqslant |k| \leqslant \alpha M} k^2 |\hat{u}_j^{(N)}|^2 = \sum_{0 \leqslant |k| \leqslant \alpha M} \hat{u}_j^{(N)*} \mathrm{i}k \left(\hat{G}_j[\mathbb{P}^{(M)} \boldsymbol{u}^{(N)}] - \hat{G}_j[\boldsymbol{u}^{(N)}]\right), \tag{27}$$

$$\begin{aligned} &-\left(\frac{\acute{\nu}_j}{M} - \frac{\bar{\nu}_j}{N}\right) \sum_{\alpha M < |k| \leqslant \beta} k^2 |\hat{u}_j^{(N)}|^2 - \left(\frac{\acute{\nu}_j}{M} - \frac{\acute{\nu}_j}{N}\right) \sum_{\beta < |k| \leqslant M} k^2 |\hat{u}_j^{(N)}|^2 \\ &\quad = \sum_{\alpha M < |k| \leqslant M} \hat{u}_j^{(N)*} \mathrm{i}k \left(\hat{G}_j[\mathbb{P}^{(M)} \boldsymbol{u}^{(N)}] - \hat{G}_j[\boldsymbol{u}^{(N)}]\right), \end{aligned} \tag{28}$$

where the repeated j indices *do not* imply a summation. These expressions for evaluating the viscosity parameters are functions of the solution itself. Thus the closed system of Eqs. (14), (11) and (27), (28) comprises a numerical method with non-linear (in $\boldsymbol{u}_N$), multiscale viscosities. In implementing this method the viscosities are evaluated based on the solution obtained from the previous time-step. However once the numerical viscosity is determined this term is treated implicitly.

7. Numerical example

As an example we apply the proposed method to Burgers equation in one dimension. In this case, in (1) and (2), $n = 1$, $\boldsymbol{f} = 0$, $\boldsymbol{G}(\boldsymbol{u}) = u^2/2$, $\boldsymbol{D} = \nu_1 = 5 \times 10^{-5}$, and $\boldsymbol{u}_0 = -\sin x$.

The solution to this problem evolves in two distinct phases. In the first phase ($t < \pi/2$), the smooth sine curve steepens. In wave number space, this corresponds to transfer of energy from the $k = 1$ mode to higher wave numbers. This phase culminates in the formation of a shock (or an inverted N-wave) at $t \approx \pi$, whose approximate width is $l = 1.6 \times 10^{-4}$ units. All the dissipation in the system is concentrated near the shock. In the wave number space, the formation of the shock corresponds to a $1/k$ spectrum that extends to the dissipation wave number, where it steepens. In the second phase, the magnitude of the N-wave reduces as $1/(1 + t)$ as the strength of the shock weakens. In wave number space, this corresponds to the lowering of the entire spectra at the rate of $1/t$. These stages of the solution are presented in Figs. 1 and 2, where we have shown a well-resolved numerical solution of the problem. Note that $E(k) \equiv |\hat{u}_k|$ represents the magnitude of the Fourier coefficients of the solution.

In order to asses the performance of the proposed method we consider the following numerical solutions:

1. A Fourier–Galerkin solution obtained by solving (10) and (11) or (12) and (13) on a fine grid in which the shock is resolved. Following terminology used in turbulence modeling we refer to this benchmark solution as the direct numerical solution (DNS). The number of modes used for computing the DNS solution is $N = 65{,}536$. This corresponds to a mesh size $h = 4.79 \times 10^{-5}$, which is smaller than the shock width $l = 1.6 \times 10^{-4}$. In Figs. 1 and 2 we have plotted this solution in physical and wave number spaces at various instances during the interval $]0, 5[$.
2. A Fourier–Galerkin solution obtained by solving (10) and (11) or (12) and (13) on a coarse grid with $N = 64$. In this case the finest resolved scale ($h = 4.9 \times 10^{-2}$) is much coarser than the scale at which dissipation occurs ($l = 1.6 \times 10^{-4}$).
3. A vanishing spectral viscosity solution on a coarse grid with $N = 64$. This method is represented by (14), where $\bar{\boldsymbol{D}} = \bar{\nu}_1 = 0$, and $\acute{\boldsymbol{D}}$ is non-zero. In particular we choose $\alpha = 1/2$ and $\acute{\boldsymbol{D}} = \acute{\nu}_1 = 0.25\alpha$. This choice for $\acute{\nu}_1$ is based on the guideline provided in [6].

4. A dynamic multiscale viscosity solution on a coarse grid with $N = 64$. This method is given by (14), where $\alpha = 1/2$ and the viscosity coefficients are determined using (27) and (28). In calculating these coefficients the solution from the previous time-step is used.

7.1. Comparison

The viscosity parameters of the dynamic multiscale method are chosen such that the method satisfies conditions that are necessary to ensure that the resulting numerical solution has the same Fourier coefficients as the continuous solution. This stipulation may be interpreted as a criterion used to design the numerical method. In the following comparison we assess how close the method comes to achieving this criterion. We also assess its performance in relation to other methods.

In Figs. 3–6, we have plotted $E(k)$ for the three numerical methods and the truncated DNS solution at four distinct times. The DNS serves as a benchmark solution. At $t = 0.5$ we observe that there is little difference in the numerical methods and the DNS. At $t = 1.5$, when the shock is about to form differences appear. A significant pile-up of energy near the cut-off wave number is observed in the coarse Fourier–Galerkin solution. For the vanishing spectral viscosity solution, this pile-up is reduced. However the solution is seen to oscillate about the DNS at wave numbers close to the separation between the coarse and fine scales ($k = 32$). The multiscale solution has much smaller oscillations at these wave numbers and only slightly underestimates the spectrum at higher wave numbers. At time $t = 2$, we observe that the pile-up at high wave numbers in the Fourier–Galerkin solution has polluted the results at lower wave numbers. The vanishing spectral viscosity solution continues to be accurate at the lower wave numbers, however the oscillations close to $k = 32$ appear to have increased. The dynamic multiscale viscosity solution is accurate at the lower wave numbers. The oscillations near $k = 32$ persist, however they are less pronounced than

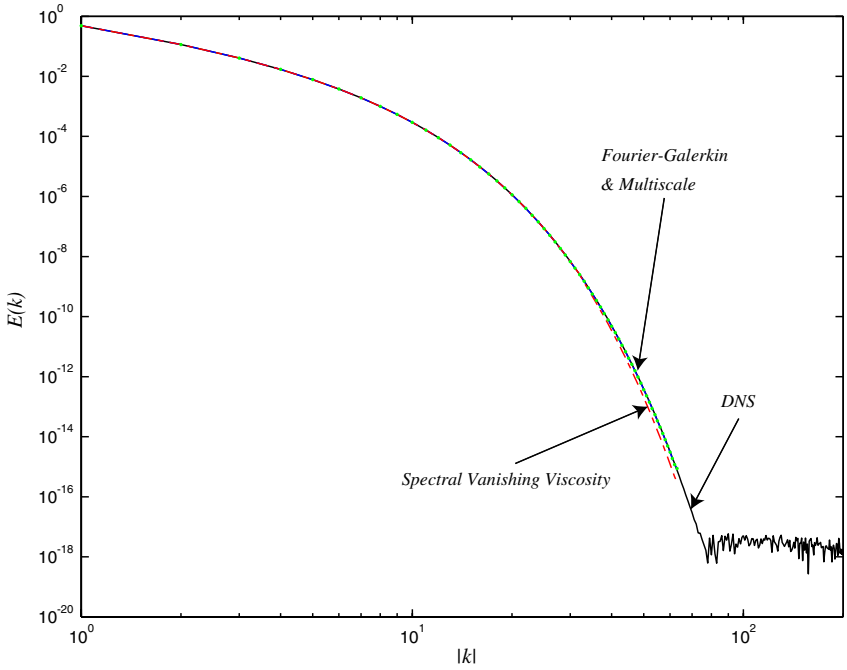

Fig. 3. $E(k)$ for the solution of the numerical methods and the DNS at $t = 0.5$.

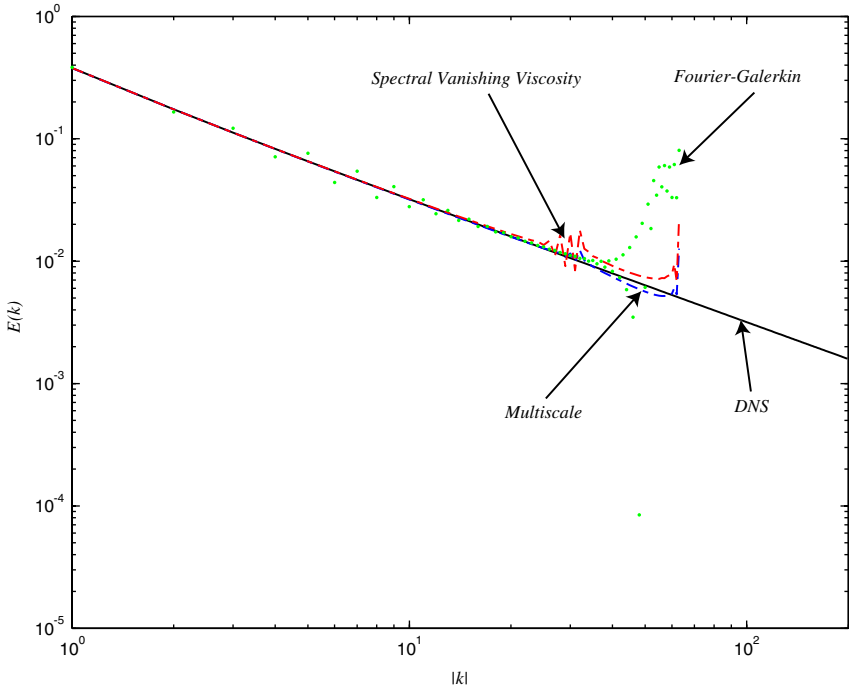

Fig. 4. $E(k)$ for the solution of the numerical methods and the DNS at $t = 1.5$.

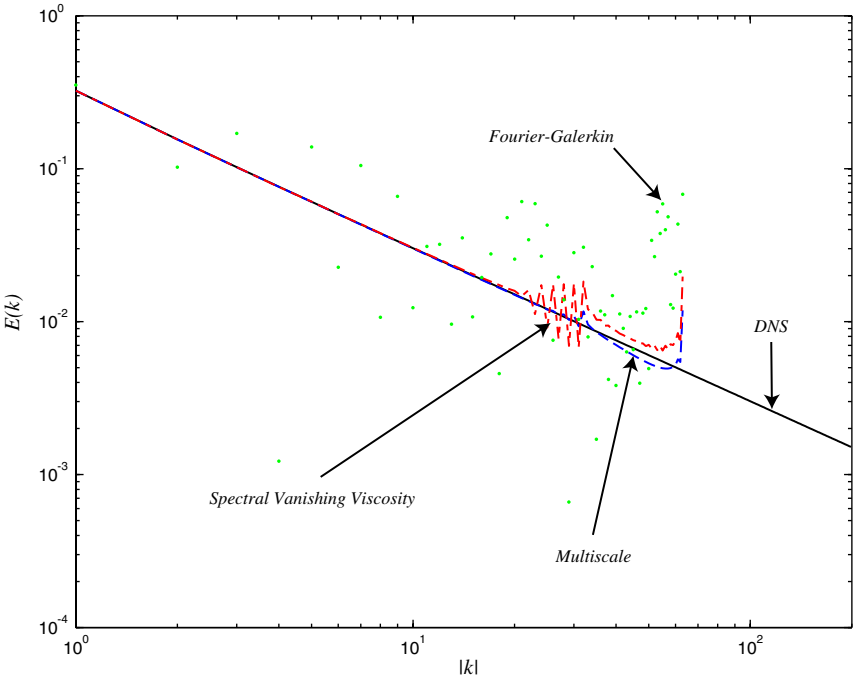

Fig. 5. $E(k)$ for the solution of the numerical methods and the DNS at $t = 2.0$.

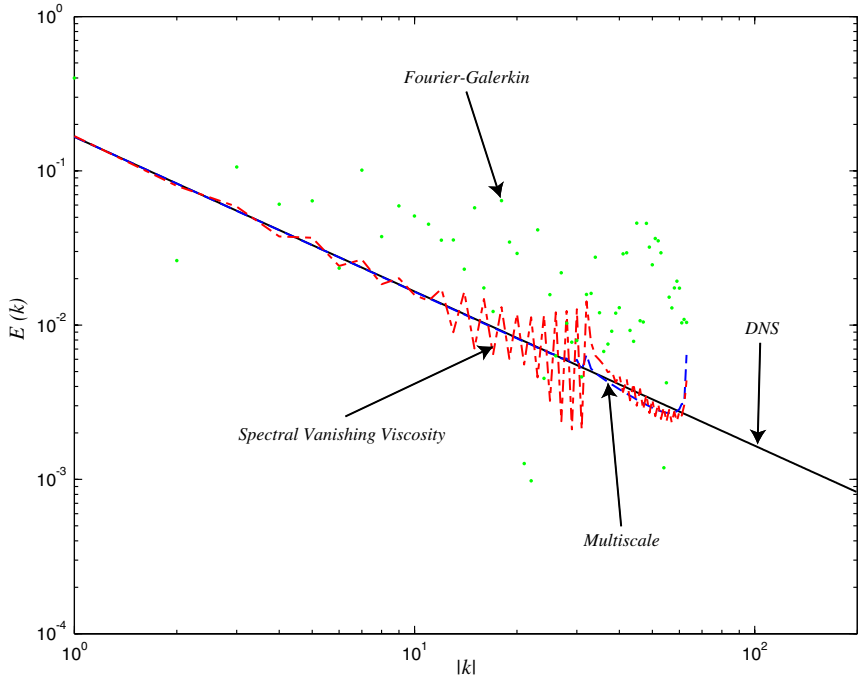

Fig. 6. $E(k)$ for the solution of the numerical methods and the DNS at $t = 5.0$.

those for the vanishing spectral viscosity solution. At $t = 5$ we observe that Galerkin solution is completely inaccurate, the oscillations in the vanishing spectral viscosity solution have increased and propagated to lower wave numbers, where as the dynamic multiscale solution has retained its accuracy.

In Fig. 7, we have plotted the viscosity parameters $\bar{\nu}_1/N$ and $\acute{\nu}_1/N$ for the vanishing spectral viscosity method and the dynamic multiscale method as a function of time. The coarse scale parameter for the vanishing spectral viscosity method is zero and is not shown, whereas the fine scale parameter which is non-zero and constant is shown. For the dynamic multiscale method we observe that both the coarse and fine scale parameters are zero till $t \approx 1$. This represents the time it takes for the energy to spill out to the wave numbers near the cut-off wave number. Thus the numerical method (correctly) imposes no viscosity till this time. Thereafter, the fine scale parameter is seen to rise, and after a while the coarse scale parameter follows suite. A couple of observations are noteworthy: (1) Unlike the vanishing spectral viscosity method, the viscosity in the coarse scales in the dynamic multiscale method is not zero, thus the method is qualitatively different. (2) The viscosity in the coarse and the fine scales is active for different periods of time, and also has different values. In particular, the fine scale viscosity is about 5/3 of the coarse scale value.

Next we compare the accuracy with which the numerical methods predict the decay of kinetic energy with time. We define the relative error in the resolved kinetic energy as follows:

$$\epsilon_{ke}(t) = \frac{\left(\sum_{|k|\leqslant 64}(\hat{\boldsymbol{u}}^{(64)})^2 - \sum_{|k|\leqslant 64}(\hat{\boldsymbol{u}})^2\right)}{\left(\sum_{|k|\leqslant 64}(\hat{\boldsymbol{u}})^2\right)}. \tag{29}$$

In Fig. 8 we have plotted $\epsilon_{ke}(t)$ for all the numerical methods. We observe that at $t \approx 1$, that is when the spectra begins to spill beyond the numerical cut-off wave number, the Fourier–Galerkin solution over-estimates the kinetic energy. By $t \approx 2.5$ its kinetic energy is about two times the actual value. Both the

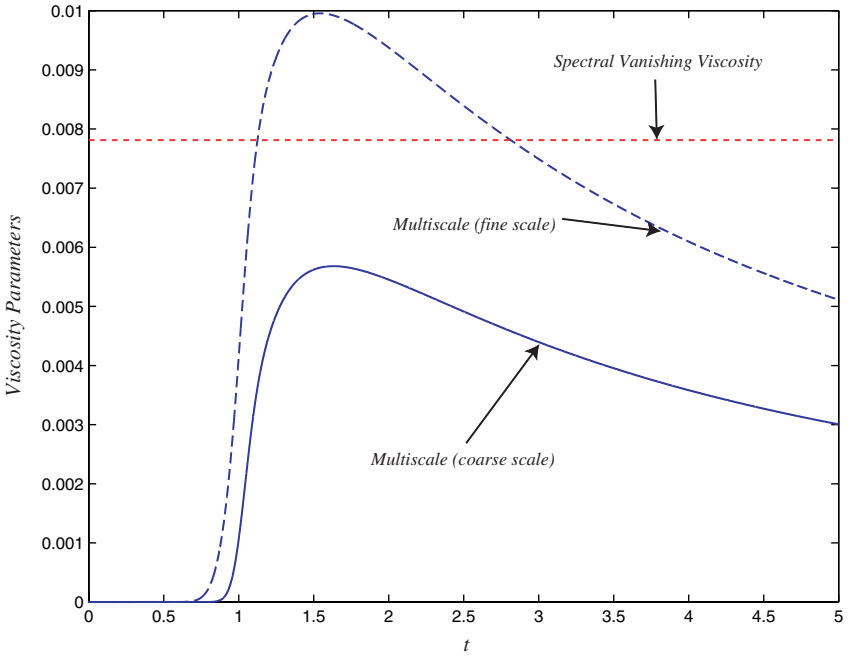

Fig. 7. Numerical viscosities for the spectral vanishing viscosity method and the dynamic multiscale method as a function of time.

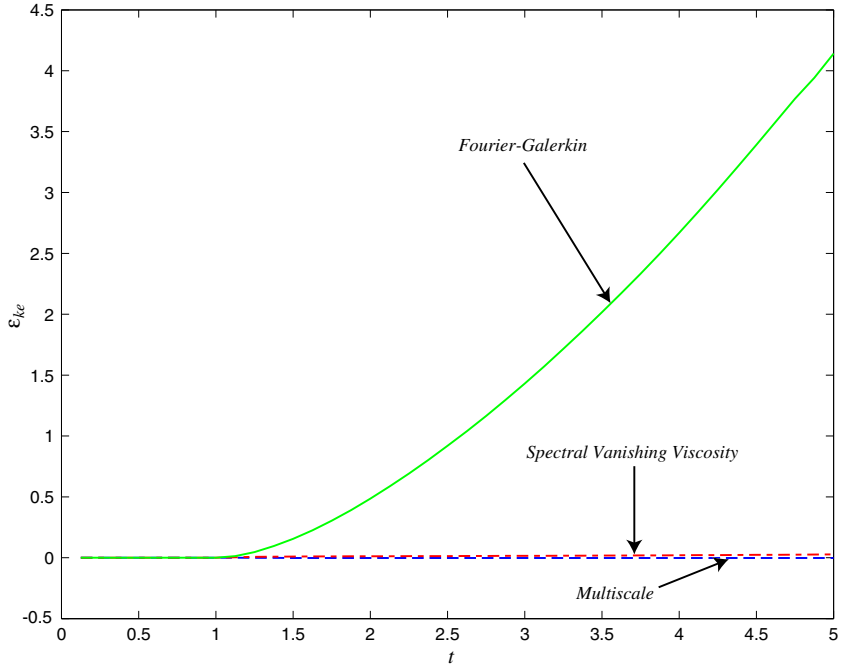

Fig. 8. Scaled error in the resolved kinetic energy of the numerical methods as a function of time.

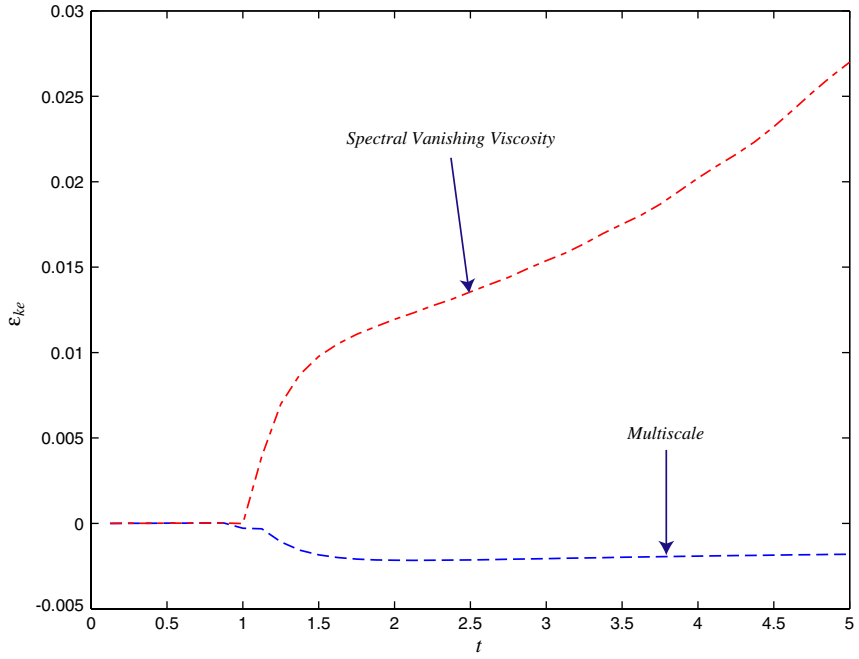

Fig. 9. Scaled error in the resolved kinetic energy of the spectral vanishing viscosity method and the dynamic multiscale method as a function of time.

vanishing spectral viscosity and the dynamic multiscale methods are much more accurate. In Fig. 9 we have compared the performance of these two methods. We observe that the vanishing spectral viscosity solution overestimates the kinetic energy and that the error is seen to increase with time. At $t = 5$ the total error is about 2.7%. The multiscale solution underestimates the kinetic energy however the error is less (about 0.2% at $t = 5$) and remarkably it does not appear to increase with time.

One of the attractive features of the vanishing spectral viscosity method is that in the limit $\nu \to 0$, it converges to the unique solution that satisfies the entropy production inequality, while *retaining spectral accuracy in the coarse modes*. This leads us to consider that while the dynamic multiscale method may be more accurate in predicting quantities such as the overall spectrum and the resolved kinetic energy, the vanishing spectral viscosity method may be more accurate in capturing the evolution of the coarse modes since it imposes no additional viscosity on these modes. In order to verify this in Fig. 10, we have plotted the error in the $k = 1$ mode, scaled by the exact value, as a function of time. That is

$$\epsilon_1(t) = \frac{\hat{\boldsymbol{u}}^{(64)}(1,t) - \hat{\boldsymbol{u}}(1,t)}{|\hat{\boldsymbol{u}}(1,t)|}. \tag{30}$$

We consider the DNS solution to be the exact value. We observe that at $t \approx \pi$ the error in the coarse Fourier–Galerkin solution rises steeply, whereas the error in the other two methods is smaller. In Fig. 11, we exclude the Fourier–Galerkin solution. We observe that error the vanishing spectral viscosity solution rises steadily beyond $t \approx 1$. At $t = 5$ the error is about 1%. The error in the dynamic multiscale method is much smaller and appears not to increase with time. At $t = 5$ it is about 0.04%. We have observed similar behavior for other coarse modes ($k = 1, \ldots, 10$). Thus contrary to what might be expected, we observe that *dynamic method* (*with a non-zero viscosity in the coarse modes*) *is more accurate than the vanishing spectral viscosity method in predicting the evolution of the coarse modes*. We attribute this observation to the

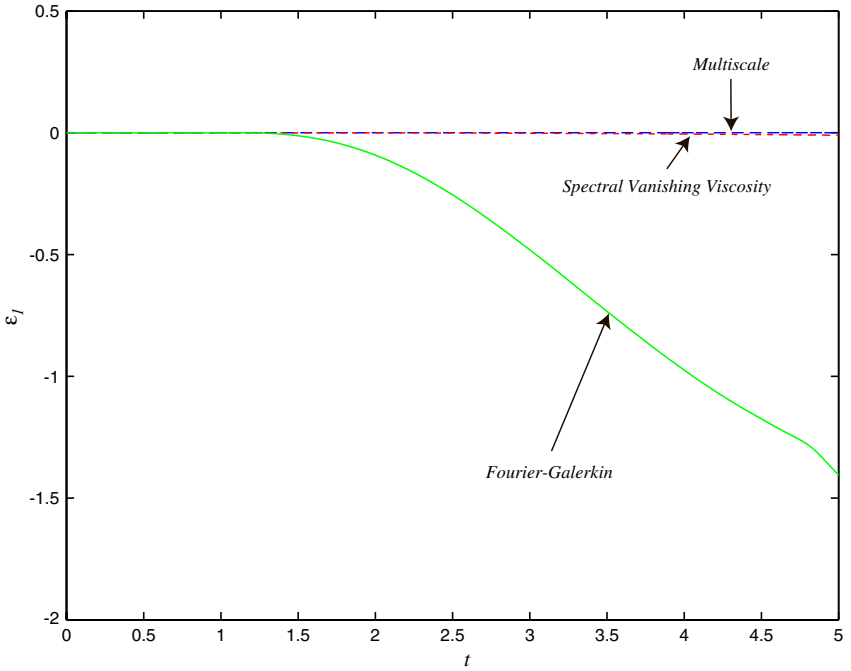

Fig. 10. Scaled error in the $k = 1$ mode of the numerical methods as a function of time.

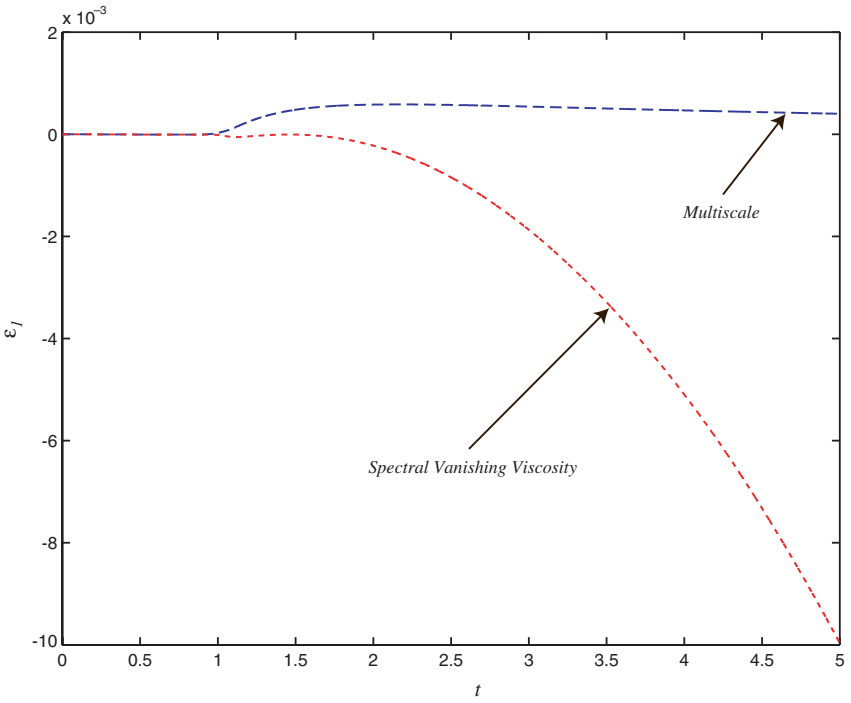

Fig. 11. Scaled error in the $k = 1$ mode of the spectral vanishing viscosity method and the dynamic multiscale method as a function of time.

hypothesis that the ideal model, which would replicate the effects of the missing scales on the retained scales exactly, may possess a non-zero viscosity at small wave numbers. We are presently verifying this hypothesis analytically and numerically.

8. Conclusions

We have proposed a new dynamic multiscale viscosity method for the spectral approximation of conservation laws in the limit of small or vanishing viscosities. Within this method the numerical approximation is split into coarse and fine scales, and likewise the projected spectral equations are also split into coarse and fine scale equations. Thereafter different numerical viscosities are applied in the coarse and fine scale equations. These viscosities are determined using a condition that must be satisfied if the resulting numerical solution is to be optimal in a user-defined sense.

We have applied this method to the one-dimensional Burgers equation. We have compared the resulting solution with the Fourier–Galerkin solution and the vanishing spectral viscosity solution computed using the same number of modes. As a benchmark we have used a well-resolved Fourier–Galerkin solution. In all comparisons we have found that the dynamic multiscale solution is the most accurate. In addition we have observed that the relative errors in this solution appear not to grow in time.

Acknowledgements

The support of ONR Grant No. 00014-02-1-0425 and DOE Award No. DE-FG02-04ER25648 is gratefully acknowledged. The DNS simulation was performed on the IBM p690 supercomputer made available through the Office of Information Technology [12] at Boston University.

References

[1] G.B. Whitham, Linear and Nonlinear Waves, John-Wiley & Sons, New York, NY, 1974.
[2] P.D. Lax, Hyperbolic systems of Conservation Laws and the Mathematical Theory of Shock Waves, Society for Industrial and Applied Mathematics, Philadelphia, PA, 1972.
[3] R.J. LeVeque, Numerical Methods for Conservation Laws, second ed., Birkhauser-Veralg, Basel, 1992.
[4] C. Canuto, M.Y. Hussaini, A. Quarteroni, T.A. Zang, Spectral Methods in Fluid Dynamics, Springer-Verlag, Berlin–Heidelberg, 1988.
[5] J. von Neumann, R.D. Richtmyer, A method for numerical calculations of hydrodynamical shocks, J. Appl. Phys. 21 (1950) 232–237.
[6] E. Tadmor, Convergence of spectral methods for nonlinear conservation laws, SIAM J. Numer. Anal. 26 (1) (1989) 30–44.
[7] T.J.R. Hughes, L. Mazzei, K.E. Jansen, Large eddy simulation and the variational multiscale method, Comput. Visual. Sci. 3 (2000) 47–59.
[8] T.J.R. Hughes, L. Mazzei, A.A. Oberai, A.A. Wray, The multiscale formulation of large eddy simulation: decay of homogeneous isotropic turbulence, Phys. Fluids 13 (2) (2001) 505–512.
[9] M. Germano, U. Piomelli, P. Moin, W.H. Cabot, A dynamic subgrid-scale eddy viscosity model, Phys. Fluids 3 (7) (1991) 1760–1765.
[10] A.A. Oberai, J. Wanderer, A dynamic approach for evaluating parameters in a numerical method, Int. J. Numer. Methods Engrg. 62 (1) (2005) 50–71.
[11] J.-L Guermond, Subgrid stabilization of Galerkin approximations of linear monotone operators, IMA J. Numer. Anal. 21 (1) (2001) 165–197.
[12] The Office of Information Technology, Boston University. Available from: <http://www.bu.edu/it/>.